Thermal Conductivity of SnTe between 100° and 500°K

D. H. Damon

Citation: Journal of Applied Physics **37**, 3181 (1966); doi: 10.1063/1.1703182
View online: https://doi.org/10.1063/1.1703182
View Table of Contents: http://aip.scitation.org/toc/jap/37/8
Published by the American Institute of Physics

Thermal Conductivity of SnTe between 100° and 500°K*

D. H. DAMON
Westinghouse Research Laboratories, Pittsburgh, Pennsylvania

(Received 15 February 1966; in final form 14 March 1966)

The thermal conductivity, electrical conductivity, and Seebeck coefficient of several specimens of SnTe have been measured between 100° and 500°K. The thermal conductivity is weakly dependent on both temperature and hole concentration. The total thermal conductivity is separated into an electronic and a lattice thermal conductivity. Because of the large concentrations of Sn vacancies in the samples, the phonons are scattered both by three-phonon umklapp processes and by the Sn vacancies; this results in a lattice thermal conductivity that varies with temperature more like $T^{-\frac{1}{2}}$ rather than T^{-1}. The Lorenz number relating the electrical conductivity and the electronic thermal conductivity is an unusual function of hole concentration. The Lorenz number is larger than the Sommerfeld value L_0, varies with hole concentration p, and has a maximum value of about 1.3 L_0 at $p=2\times10^{20}$ cm^{-3}. This is consistent with the variation of the electrical conductivity and the Seebeck coefficient with hole concentration.

INTRODUCTION

THE theory of the heat transport by lattice waves in solids at high temperatures when the phonon mean free path is limited both by three phonon collisions and by collisions of the phonon with point imperfections has been developed by Klemens,[1] Callaway,[2] Ambegaokar,[3] and Parrot.[4] Klemens, Tainsh, and White[5] found that the theory correctly predicted some of the characteristics of the thermal conductivity of Cu and Ag alloys. It has been used to interpret measurements of the thermal conductivity of Ge–Si alloys[6] and a number of other heavily doped semiconductors.[7] Vishnevskii and Sukharevskii[8] studied the effect of foreign cations and cation vacancies on the thermal conductivity of MgO at high temperatures.

Most of the previous investigations have been concerned with the effect of substitutional foreign atoms. The aim of the present investigation was to study the applicability of the theory to the scattering of phonons by vacancies at high temperatures. For this purpose SnTe would seem to be an ideal material. Two independent investigations[9,10] have established that SnTe prepared at high temperatures and normal pressures is nonstoichiometric, being deficient in Sn. The Sn vacancies act as doubly charged acceptors and the true hole concentration p is related to the value of the Hall constant at 77°K, R_{77}, by $p=0.6/R_{77}e$.[11] Therefore, the Sn vacancy concentration $[V_{Sn}]$ can be simply determined by measuring the Hall constant. Moreover, $[V_{Sn}]$ can be varied over a fairly wide range of values (from $\sim5\times10^{19}$ to $\sim5\times10^{20}$ cm^{-3}) by heat treating the samples in either Te-rich or Te-deficient atmospheres.[10,12] In this way one can study the effect of a known and variable vacancy concentration on the lattice thermal conductivity.

In order to study the lattice thermal conductivity, one must subtract the electronic component from the measured thermal conductivity; the electronic component is related to the electrical conductivity σ by the relation $\kappa_e=L\sigma T$, where L is the Lorenz number. Unfortunately, the Lorenz number depends on the electronic band structure, and may depart from the Sommerfeld value appropriate for the highly degenerate case of a metal. The principal features of the band structure of SnTe seem to be well established[13,14]; it is a semiconductor with two overlapping valence bands, the band edges being separated by a few tenths of an electron volt. However, the electrical conductivity, the Seebeck coefficient and the Hall coefficient are not fully understood quantitatively. In particular, the Seebeck coefficient shows an unusual dependence on hole concentration.[13] At room temperature the Seebeck coefficient first decreases as p increases reaching a minimum value for $p\approx1.5\times10^{20}$ cm^{-3} and then increases to a maximum value for $p\approx5\times10^{20}$ cm^{-3}. As p is further increased, the Seebeck coefficient again decreases. Brebrick and Strauss[15] have published a detailed analysis of the Seebeck coefficient using the two-valence band model. Although their model reproduced the qualitative features of the observed variation of the Seebeck coefficient with hole concentration, it was quantitatively unsatisfactory. In particular, it could

* Sponsored in part by the U. S. Air Force Office of Scientific Research.

[1] P. G. Klemens, Phys. Rev. **119**, 507 (1960).
[2] J. Callaway, Phys. Rev. **113**, 1046 (1959).
[3] V. Ambegaokar, Phys. Rev. **114**, 488 (1959).
[4] J. E. Parrot, Proc. Phys. Soc. (London) **81**, 726 (1963).
[5] P. G. Klemens, G. K. White, and R. J. Tainsh, Phil. Mag. **7**, 1323 (1962).
[6] B. Abeles, Phys. Rev. **131**, 1906 (1963).
[7] J. R. Drabble and H. J. Goldsmid, *Thermal Conduction in Semiconductors* (Pergamon Press, Inc., New York, 1961).
[8] I. I. Vishnevskii and B. Ya. Sukharevskii, Soviet Phys.—Solid State **6**, 1708 (1965).
[9] R. Mazelsky and M. Lubell, Advan. Chem. Ser. **39**, 210 (1963).
[10] R. F. Brebrick, J. Phys. Chem. Solids **24**, 27 (1963).
[11] B. B. Houston, R. S. Allgaier, J. Babiskin, and P. G. Siebenmann, Bull. Am. Phys. Soc. **6**, 60 (1964).
[12] A. Sagar and R. C. Miller, in *Proceedings of the 1962 International Conference on Physics of Semiconductors, Exeter*, A. C. Stickland, Ed. (The Institute of Physics and The Physical Society, London, 1962).
[13] J. A. Kafalas, R. F. Brebrick, and A. J. Strauss, Appl. Phys. Letters **4**, 93 (1964).
[14] J. R. Burke, Jr., R. S. Allgaier, B. B. Houston, J. Babiskin, and P. G. Siebenmann, Phys. Rev. Letters **14**, 360 (1965).
[15] R. F. Brebrick and A. J. Strauss, Phys. Rev. **131**, 104 (1963).

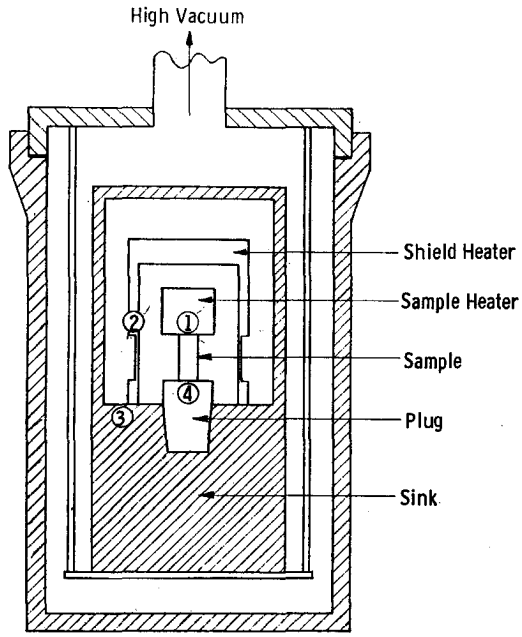

FIG. 1. Schematic drawing of the apparatus. The encircled numbers locate the positions of 4 copper–constantan thermocouple beads. The temperature difference between 1 and 2 is reduced to zero by adjusting the shield heater. The temperature differences 2–3 and 3–4 are measured. The chamber is evacuated to a pressure of $\sim 10^{-5}$ Torr and is immersed in a suitable temperature bath. A heater wrapped on the sink is used to reach intermediate temperatures.

not explain the very small minimum value of S. This small minimum can be understood if one is willing to assume that another scattering mechanism is present.

Even though one does not yet understand the scattering mechanism which causes the observed dependence of the Seebeck coefficient on hole concentration, one can relate the Lorenz number, the Seebeck coefficient, and the electrical conductivity in a phenomenological manner. It is shown that this variation implies a departure of the Lorenz number from the Sommerfeld value, depending on p and reaching a maximum value for a value of p of about 2×10^{20} cm^{-3}.

The thermal conductivity, electrical resistivity, and Seebeck coefficient of four samples of SnTe were measured between 100° and 500°K. Since we do not know the Lorenz number, we cannot effect a unique separation of the thermal conductivity into electronic and lattice components. However, we know from theory that departures from the Sommerfeld value are least at lowest temperature, and using this value at 100°K we obtain values of the lattice thermal conductivity which show a proper dependence on vacancy concentration. Extrapolating these values to higher temperatures we deduce the electronic thermal conductivity and the Lorenz number. We find that this procedure, while not absolutely certain, does lead to self-consistent results and that the measured thermal conductivity can be understood in terms of: (1) a lattice thermal conductivity determined by a combination of three-phonon umklapp processes and point-defect scattering which turns out to be strong for vacancies in SnTe; and (2) a Lorenz number whose dependence on hole concentration is consistent with the behavior of other transport properties of SnTe.

EXPERIMENTAL PROCEDURE

Figure 1 is a schematic drawing of the apparatus used to measure the electrical resistivity ρ, thermal conductivity κ, and Seebeck coefficient S, of SnTe. The samples, rectangular parallelepipeds about $1\times 0.3\times 0.3$ cm, were soldered between the plug and the sample heater. Temperatures were measured with four copper–constantan thermocouples located as shown in the drawing. The thermal conductivity was measured by the standard stationary-heat-flow method.[16]

Bauerle[17] has discussed the use of this apparatus in detail. The heat flux through the sample was calculated from the power generated in the heater corrected for any small drift of the average temperature and for the radiative transfer. The thermal resistance of the solder layers[17] was subtracted from the total measured thermal resistance to obtain the thermal resistance of the sample. Measurements of pure germanium have been made with this apparatus in order to check the reliability of the correction for the thermal resistance of the solder layer. These results showed that the error due to uncertainty in this correction could be kept below 5% for samples with thermal conductivities as large as 2 W·cm^{-1} °K^{-1} provided that the electrical resistance of the solder–sample contact could be kept very small. For this reason the electrical resistivity of the SnTe samples was first measured using a four-probe technique and then remeasured in the thermal conductivity apparatus. The difference between the results of the four-probe and two-probe measurements never exceeded 2%, most of which could be ascribed to uncertainties in the determination of sample geometry. The values of κ given below are accurate to $\pm 2\%$ except possibly at the highest temperatures where the correction for the radiative transfer was about 15% of the total heat flow.

The radiative heat transfer was studied as a function of the area of the surface of the sample, the emissive character of the surface, the temperature, and the temperature difference $\Delta T = T_1 - T_4$ (see Fig. 1). Measurements were made on two specimens by the stationary heat flow method. One specimen was a stainless steel (No. 304) spool. The disks forming the ends of the spool were soldered to the heater and plug. The rod forming the barrel of the spool was 0.56 mm in diameter and 1.1

[16] N. Pearlman, in *Methods of Experimental Physics*, K. Lark-Horovitz and V. A. Johnson, Eds. (Academic Press Inc., New York, 1959), Vol. 6A.

[17] J. E. Bauerle, in *Thermoelectricity, Science and Engineering*, edited by R. R. Heikes and R. W. Ure, Jr. (Intersceince Publishers, Inc., New York, 1961).

cm long. The area of the rod from which heat could be radiated was therefore about 0.2 cm², considerably smaller than the surface area of a typical SnTe specimen (~1.2 cm²). At 420°K the total thermal conductance was 1.78×10^{-3} W °K^{-1}; of this 0.34×10^{-3} W °K^{-1} was due to conductance through the stainless steel rod.

A second sample was fabricated from a hollow stainless steel cylinder 1.3 cm long and 1.23 cm in diameter with a wall thickness of 6×10^{-3} cm. The cylinder was filled with powdered ZrO_2. A small hole was drilled through the wall of the cylinder so that the air would be removed. In a separate experiment it was found that the effective thermal conductivity of this powder, loosely packed in a vacuum, was 3×10^{-5} W·cm^{-1} °K^{-1}. The heat transported through the ZrO_2 powder was therefore negligible compared to that conducted through the stainless steel. The surface area of this sample from which heat would be radiated was about 5 cm², considerably larger than the area of a typical SnTe specimen. This specimen was first measured with its outer surface gold-plated (thickness, $\sim2\times10^{-5}$ cm); it was then remeasured after being blackened with soot from an acetylene flame.

Measurements on these samples were carried out between 300° and 500°K. Some difficulty was encountered since a typical time constant for the sample and heater is 2×10^3 sec. Measurements were made at intervals of about 20 min for a period of about 4 h after the apparatus had reached stationary conditions. For both specimens the total measured thermal conductance, K, could be represented by $K=K_0+cT^3$ independent of ΔT for $1°K<\Delta T<5°K$. This has an obvious interpretation: K_0 represents the conductance through the stainless steel and cT^3 is the conductance due to radiation. This relation cannot be exact since the thermal conductivity of stainless steel is feebly temperature-dependent. However, the experimental accuracy did not permit further analysis. The values of K_0 yielded values of the thermal conductivity of No. 304 stainless steel in reasonably good agreement with previously published values considering, for example, the difficulty of making an accurate measurement of the wall thickness of the cylinder. The value of c was 1.3 times larger for the gold-plated hollow cylinder than for the thin rod. It was about 1.1 times larger for the blackened cylinder than for the gold-plated cylinder. The measurements made on the thin rod were assumed to give the heat radiated from the heater to the sink. The differences between these measurements and the measurements made on the thin-walled cylinder then gave the heat radiated from the surface of the cylinder. In this way one finds that the heat radiated from the blackened surface was only about 1.5 times greater than the heat radiated from the gold surface. This small difference is perhaps not surprising remembering that the gold layer was very thin and not polished. The average of the values found for the two surfaces was used for SnTe. This is, of course, uncertain. However, since we have shown that the fraction of the total radiative heat transfer due to radiation from the surface of the samples is small this uncertainty should not introduce appreciable error. The low-temperature radiation corrections were found by extrapolation.

TABLE I. Values of the Hall coefficient R_{77}, electrical conductivity σ_{77} at 77°K, and the Sn vacancy concentration $[V_{Sn}]$, for each of the samples.

Sample	R_{77} (cm³ C^{-1})	σ_{77} (Ω^{-1} cm^{-1})	$[V_{Sn}]\times10^{-19}$ (cm^{-3})
a	2.34×10^{-2}	2.4×10^4	7.9
b	1.81×10^{-2}	2.0×10^4	10.3
c	7.9×10^{-3}	2.1×10^4	24
d	3.12×10^{-3}	1.7×10^4	60

Measurements were also made with the thermal shield unbalanced. At 485°K it was found that increasing T_1-T_2 (see Fig. 1) from 0°K (actually <0.01°K) to 0.4°K increased the radiative heat transfer by 35%. This shows the effectiveness of the thermal shield.

Measurements of the heat radiation were also made dynamically. For example, without any specimen in the chamber the heater was suspended from the shield on a thread. After stationary conditions were reached with $\Delta T=6°K$ and $T_1-T_2=0$ the sample heater was turned off and ΔT was measured as a function of time. These results were unsatisfactory. It was found to be difficult to keep T_1-T_2 equal to zero and to prevent the sink temperature, T_3, from decreasing.

These special test samples do not perfectly reproduce the environment of the SnTe samples, and some uncertainties remain. As previously mentioned, the correction for the radiative transfer was only about 15% of the total heat flow at 500°K; therefore, it does not seem likely that these uncertainties would introduce more than 1% or 2% error into the thermal conductivity of SnTe.

Single-crystal SnTe is very brittle; if the samples are soldered to a copper heater and plug they break up upon cooling to 77°K. It was found that over the temperature range 100° to 500°K the thermal expansion of aluminum was, quite fortuitously, a fair match to that of SnTe. It required some care to eliminate the electrical resistance at the solder–aluminum contacts; however, this was successfully accomplished using 75Pb–25Sn solder and Aluten 51B flux manufactured by Eutectic Welding Alloys Corporation, New York, New York.

The samples were cut from the same single-crystal ingot in the form of rectangular parallelepipeds $1\times0.5\times0.5$ cm. Each sample was heat treated in an appropriate atmosphere,[10,12] in some cases for as long as 1300 h, to produce a sample with a desired hole concentration. Homogeneity was checked by reducing the sample to $1\times0.3\times0.3$ cm by a succession of lappings. Between lappings the Seebeck coefficient was measured at room temperature and was found to be independent of the size of the sample. After all measurements were

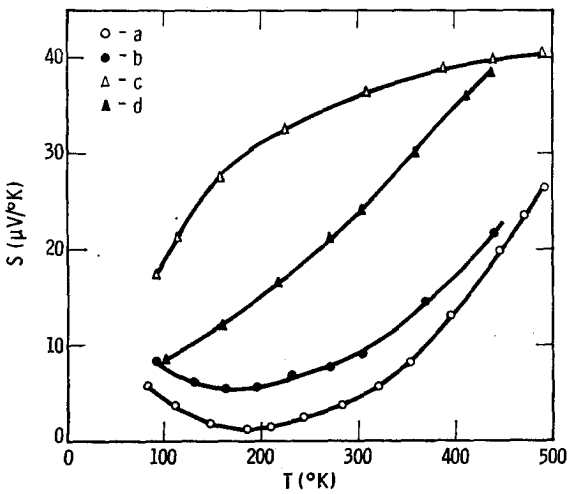

FIG. 2. Measured values of the Seebeck coefficient S plotted against temperature T for each of the samples.

completed, each sample was sliced into three bars and Hall coefficient measurements were made. These measurements also showed that the samples were homogeneous; for example, for sample b Hall constant values of 1.86, 1.76, and 1.85×10^{-2} cm^3 C^{-1} were found. Table I lists the values of the Hall coefficients and electrical conductivities at 77°K and the Sn vacancy concentration for each sample.

EXPERIMENTAL RESULTS

In Fig. 2 the measured values of the Seebeck coefficients S are plotted against temperature. These results are in excellent agreement with previously published values.[12,13,15] The measured values of the thermal conductivity κ are plotted against temperature in Fig. 3. Also shown in this figure are the values of $\kappa_e' = (\pi^2/3)(k/e)^2\sigma T$, the Wiedemann–Franz law electronic thermal conductivity for a degenerate gas of holes, calculated from the measured values of the electrical conductivity. Figure 4 shows the difference, $\kappa-\kappa_e'$, plotted against absolute temperature. For samples a and b, $\kappa-\kappa_e'$ decreases with increasing temperature slightly faster and considerably slower, respectively, than $T^{-0.5}$. The difference between the values of $\kappa-\kappa_e'$ for samples a and b should be particularly noted. Sample b contains only about 30% more holes and vacancies than sample a. Consistent with this difference in vacancy concentration, assuming that the vacancies scatter phonons, the value of $\kappa-\kappa_e'$ for sample a at 100°K is slightly larger than it is for sample b. However, at 500°K the value of $\kappa-\kappa_e'$ for sample a is considerably smaller than it is for sample b. This result certainly suggests that the quantity $\kappa-\kappa_e'$ is not the true lattice thermal conductivity for all the samples throughout the temperature range 100° to 500°K. In Fig. 5, $\kappa-\kappa_e'$ at 100°K is plotted against $[V_{Sn}]$; at this temperature $\kappa-\kappa_e'$ is proportional to $[V_{Sn}]^{-\frac{1}{3}}$.

In order to be sure that the lengthy heat treatments of samples a, b, and d did not produce changes in the lattice (other than changing the vacancy concentration) which would affect the lattice thermal conductivity, an untreated single-crystal sample was annealed for 1300 h at 873°K (about 80% of the melting temperature).

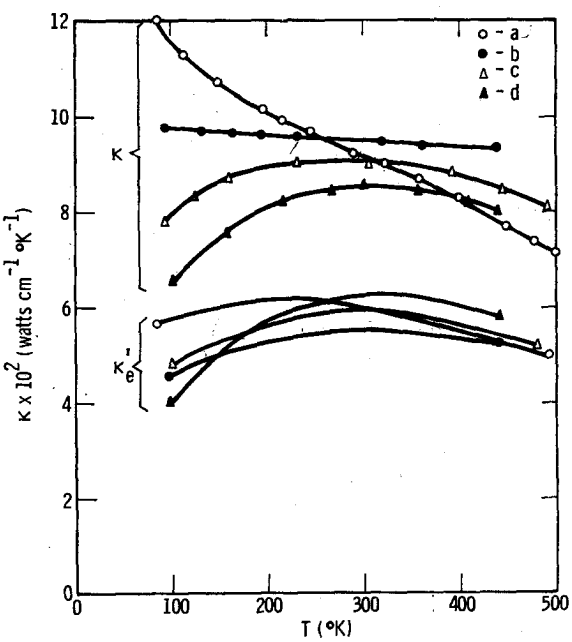

FIG. 3. Measured values of the thermal conductivity κ and the Wiedemann–Franz law electronic thermal conductivity, $\kappa_e' = (\pi^2/3)(k/e)^2\sigma T$, calculated from the measured electrical conductivity σ plotted against temperature.

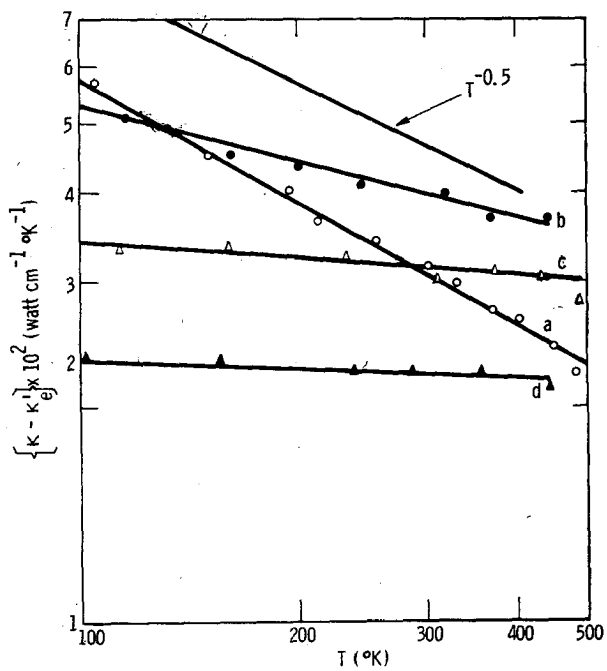

FIG. 4. The difference between the measured thermal conductivity and $\kappa_e' = (\pi^2/3)(k/e)^2\sigma T$, $\kappa-\kappa_e'$, plotted against temperature.

Table II shows that the electrical resistivity, the thermoelectric power, the Hall coefficient, and the thermal conductivity were all unaffected by this annealing. Therefore, the differences between the thermal conductivities of these samples can be attributed to the differences between their vacancy and hole concentrations.

DISCUSSION

We first show that for SnTe the Debye temperature θ_D is approximately 130°K and that, therefore, high-temperature approximations can be used to discuss the results of this investigation. The Klemens theory of lattice thermal conductivity is then used to explain the temperature dependence of $\kappa-\kappa_e'$ for sample a and the result $\kappa(100)-\kappa_e'(100)\propto[V_{\mathrm{Sn}}]^{-1}$. Finally, the difference between the thermal conductivities of samples a and b is shown to be a result of the variation of the Lorenz number with hole concentration.

A. Model for the SnTe Lattice

In the absence of specific heat data one might hope to estimate a value of θ from measurements of the elastic constants according to[18]

$$\theta_B\approx 0.7(h/k)(B/\rho)^{\frac{1}{2}}(3/4\pi V_m)^{\frac{1}{3}}, \qquad (1)$$

where B is the bulk modulus, ρ the density, and V_m the volume occupied by one molecule. Houston and Strakna[19] have shown that the elastic constants of SnTe vary with p. However, B is only weakly dependent on p and the use of $B=4.2\times10^{11}$ dyn/cm^{-2} found by them for a sample with $(R_{77}e)^{-1}=1.24\times10^{20}$ should provide a reasonably reliable estimate of θ_D. Using $V_m=6.31\times10^{-23}$ cm^{-3} computed by using 6.32 Å for the lattice parameter of the fcc cell, Eq. (1) yields $\theta_B\approx130$°K. Alternatively, B might be eliminated in favor of the melting temperature T_m by use of the relation[18]

$$T_m\approx BV_mN_0/8\gamma^2C_v, \qquad (2)$$

where γ is the Grüneisen constant, N_0 is Avogadro's number, and C_v is the heat capacity per mole of SnTe. Using $\gamma=2.0$ and $C_v=6R$, Eq. (2) yields $T_m\approx1000$°K which may be compared to the measured maximum melting temperature of SnTe,[10] 1079°K. It is clear that the use of T_m will yield nearly the same value of θ_D. Bolef's measurements[20] of the coefficient of linear thermal expansion α provide further information about θ_D. He found α to be 2.0×10^{-5} (°K)$^{-1}$ at room temperature and to decrease to half this value at about 25°K. This suggests that θ_D is not much greater than 100°K. This value of α together with $B=4.2\times10^{11}$ dyn/cm^{-2} yields $\gamma=(3B\alpha V_mN_0)/C_v=1.95$. The available experimental data, therefore, suggest that the SnTe lattice be described in terms of the following parameters: $\theta_D=130$°K, $\gamma=2.0$, and $V_m=6.3\times10^{-23}$ cm^{-3} which defines a "lattice constant," $a^3=V_m$ or $a\approx4\times10^{-8}$ cm, and a spherical Brillouin zone $(4\pi/3)(q_D/2\pi)^3=V_m^{-1}$ with $q_D\approx10^8$ cm^{-1}, the wavenumber at the Debye cutoff.

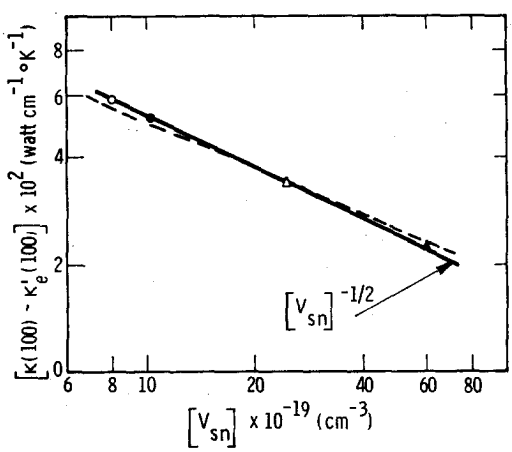

FIG. 5. The difference between the measured thermal conductivity and $\kappa_e'=(\pi^2/3)(k/e)^2\sigma T$ at 100°K, $\kappa(100)-\kappa_e'(100)$, plotted against Sn vacancy concentration $[V_{\mathrm{Sn}}]$. The dashed curve shows the best fit of Eq. (3) to the data if $\kappa_u=13T^{-1}$ W·cm^{-1} °K^{-1} is the lattice thermal conductivity of stoichiometric SnTe at $T>\theta\approx130$°K.

TABLE II. An untreated single-crystal sample cut from an ingot pulled from a stoichiometric melt of SnTe was annealed at 873°K for 1300 h. Values of the Hall coefficient R, electrical resistivity ρ, thermoelectric power S, and thermal conductivity κ, show that annealing SnTe without changing the vacancy concentration does not change the thermal conductivity.

T (°K)	ρ (Ω·cm)	S (μV/°K)	κ [W/(cm deg)]	R [cm³/C]
Before annealing				
~300	12.5×10^{-5}	35.9	0.091	···
100	5.1×10^{-5}	19.0	0.080	$+7.8\times10^{-3}$
After annealing				
~300	12.4×10^{-5}	36.5	0.093	···
100	5.2×10^{-5}	19.4	0.079	$+7.5\times10^{-3}$

B. Lattice Thermal Conductivity

For $T>\theta$ we assume that the phonon scattering by holes is negligible[21] and the phonon mean free path is limited by three-phonon umklapp processes and by point-defect scattering. Combining the effects of both scattering processes, Klemens[1] obtained for the lattice

[18] C. Zwikker, *Physical Properties of Solid Materials* (Interscience Publishers, Inc., New York, 1954), Chap. IX.

[19] B. B. Houston and R. E. Strakna, Bull. Am. Phys. Soc. **9**, 646 (1964).

[20] D. Bolef (private communication).

[21] J. M. Ziman, *Electrons and Phonons* (Oxford University Press, London, 1960), p. 319 ff.

thermal conductivity κ_L, the formula

$$\kappa_L=\kappa_u(\omega_0/\omega_D)\tan^{-1}(\omega_D/\omega_0) \tag{3}$$

with

$$\frac{\omega_0}{\omega_D}=\left[\frac{2}{\pi}\frac{kv}{a^3q_DnS^2\kappa_u}\right]^{\frac{1}{2}}, \tag{4}$$

where ω_D is the Debye frequency, v the velocity of sound, n the fractional concentration of point defects ($n=[V_{Sn}]V_m$ for SnTe), S^2 is a parameter describing the strength of the point-defect scattering, and κ_u is the lattice thermal conductivity of the perfect crystal. In the limit of strong point-defect scattering $[(\omega_0/\omega_D)\rightarrow 0]$, Eq. (3) becomes

$$\kappa_L=\kappa_u(\omega_0/\omega_D)(\pi/2). \tag{5}$$

Substituting the values of v, a^3, and q_D given above, we have

$$\frac{\omega_0}{\omega_D}=\frac{6.22\times10^{12}}{S[V_{Sn}]^{\frac{1}{2}}\kappa_u^{\frac{1}{2}}} \tag{6}$$

and

$$\kappa_L=9.8\times10^{12}\,\kappa_u^{\frac{1}{2}}/S[V_{Sn}]^{\frac{1}{2}}. \tag{7}$$

Since we expect $\kappa_u\propto T^{-1}$ at these temperatures, Eq. (7) accounts for the temperature dependence of $\kappa-\kappa_e'$ for sample a and for $\kappa(100)-\kappa_e'(100)\propto[V_{Sn}]^{-\frac{1}{2}}$ (Fig. 5). Using the data shown in Fig. 5, Eq. (7) yields $\kappa_u^{\frac{1}{2}}/S=5.4\times10^2$ erg$^{\frac{1}{2}}$ cm$^{-\frac{1}{2}}$ sec$^{-\frac{1}{2}}$. We must attempt to estimate values of κ_u and S to see if this value of $\kappa_u^{\frac{1}{2}}/S$ is reasonable and to find out if the condition $\omega_0/\omega_D\ll1$ is satisfied.

Using $\theta_D\approx130$°K, κ_u may be calculated from the Leibfried-Schloemann formula[22]

$$\kappa_uT\approx0.95(k/h)^3Ma\theta^3\approx31\ \text{W}\cdot\text{cm}^{-1},$$

where M is the mass of one molecule of SnTe. It is known[23] that this expression yields values of κ_uT that are larger than experimental values by a factor between 2 and 3 for the elements and for binary compounds whose constituents have nearly equal masses. Therefore, the value of κ_uT probably lies between 10 and 15 W·cm^{-1}. Another estimate of κ_uT may be obtained from Keyes[24] semiempirical formula relating κ_uT to $T_m^{3/2}\rho^{2/3}A^{-7/6}$, where A is the mean atomic mass. For SnTe this yields $\kappa_uT\approx13$ W·cm^{-1} which, as Keyes points out, may be too small (large) by a factor four (two) if the bonding is purely covalent (ionic). These considerations suggest that $\kappa_uT=13$ W·cm^{-1} is a reasonable value for stoichiometric SnTe. Together with our previous result this requires $S^2=4.4$ and $\omega_0/\omega_D=0.29$ for sample a at 100°K. The approximation $\omega_0/\omega_D\ll1$ is therefore not fully justified. Using $\kappa_u=13\ T^{-1}$ W·cm^{-1} deg^{-1}, Eq. (3) was fit to the measured values of $\kappa(100)-\kappa_e'(100)$ with a constant value of $S^2=3.3$. This fit is shown by the dashed curve in Fig. 5.

According to Klemens,[25] point-defect scattering may be considered to be the combined effects of scattering due to the mass difference S_1, the change in the force constants at the defect site S_2, and the strain field caused by the dilation or contraction of the lattice about the defect S_3. The scattering parameter S^2 represents the total point-defect scattering and is given by $S^2=S_1^2+(S_2+S_3)^2$. The strength of the scattering due to the mass difference is measured by[26] $S_1=\Delta M/M\approx\frac{1}{2}$, where ΔM is the change in the mass of a SnTe molecule upon introducing a Sn vacancy and M is the mass of the molecule.[27] Therefore if $S^2\approx3$, then only a small fraction of this can be accounted for by the mass difference. The effect of the change in the force constants upon introducing a vacancy is difficult to calculate but a crude estimate of the effect of the strain field may be obtained. S_3 which represents the scattering due to the strain field surrounding the temperature is given by[25]

$$S_3^2\approx3\times10^2(\Delta R/R)^2,$$

where ΔR is the displacement of each of the atoms nearest to the vacancy caused by the introduction of the vacancy and R is the nearest-neighbor distance.

The lattice parameter of SnTe decreases linearly with Sn vacancy concentration[9,10,12] from $a=6.323$ Å for $[V_{Sn}]=7\times10^{19}$ cm^{-3} to $a=6.297$ Å for $[V_{Sn}]=5.3\times10^{20}$ cm^{-3}; therefore there is some reason to expect that an appreciable strain field surrounds each vacancy. Vegard's law may be used to obtain a rough estimate of $\Delta R/R$. We assume the following: Each complete molecule occupies a volume V_m, each defective molecule, i.e., each unpaired Te atom, occupies a volume V_d, and the third power of the measured lattice parameter is a weighted average of these volumes. A simple calculation then yields $(V_m-V_d)/V_m$. If $\Delta R/R$ is one-third of this quantity, then one finds $(\Delta R/R)^2\approx0.016$ and $S_3^2\approx4.8$. While this suggests that S^2 may well have a value of 3 for vacancies in SnTe, it must be noted that the calculation probably overestimates $\Delta R/R$ and moreover the term S_2S_3 that appears in S^2 should be negative[25] for a vacancy with $\Delta R/R<0$.

Klemens' theory therefore provides a partial account of the experimental values of $\kappa-\kappa_e'$. The data establish

[22] G. Leibfried and E. Schloemann, Nockr. Akad. Weiss. Göttingen, Math.-Phys. Kl. **2a**, No. 4, 71 (1954). The expression given in the text was taken from Ref. 23.

[23] P. G. Klemens, Solid State Phys. **7**, 1 (1958).

[24] R. W. Keyes, Phys. Rev. **115**, 564 (1959).

[25] P. G. Klemens, Proc. Phys. Soc. (London) **A68**, 1113 (1955).

[26] This expression is taken from Ref. 1 and differs from that in Ref. 25 by a factor $2\sqrt{3}$.

[27] Throughout this discussion we have treated the SnTe lattice as having two atoms per unit cell. Considering the near equality of the masses of Sn and Te, one might also use a monatomic cell. This will make very little difference (factors of $2^{1/3}$ or $2^{1/6}$ in some of the expressions) since the theory is strictly applicable only to an elastic continuum, i.e., in the long-wavelength limit. The details of the construction of the cell do not matter much so long as one keeps the correct number of vibrational modes and maintains a consistent viewpoint. In using the monatomic cell, V_m, a, q_D, and n would have different values and one would find a different value of S^2 in fitting Eq. (3) to the data. One would then take $S_1=1$.

a value of κ_u/S^2 which is consistent with reasonable values of κ_u and S^2. Obviously there is some freedom in choosing κ_u and S^2 (keeping κ_u/S^2 constant) but this freedom is not unlimited. In particular, one cannot choose considerably smaller values of both κ_u and S^2; otherwise the condition $\omega_0/\omega_D<1$ would not be satisfied and the theory would not yield $\kappa_L \propto [V_{\mathrm{Sn}}]^{-\frac{1}{3}}$.

It must be mentioned that there are serious objections to the use of this theory. The theory assumes that the point defects are randomly distributed. The vacancy concentrations are large (approaching 4% for the sample with the largest hole concentration). It would not be unreasonable to expect at least partial ordering of the vacancies. The effect of N-processes has been ignored. Parrot[28] has described the effect of N-processes at high temperatures; however, in view of the uncertainties that are encountered in the next section, it did not seem worthwhile to pursue these questions.

C. The Electronic Thermal Conductivity

The formula[29] for the electrical conductivity of a cubic crystal,

$$\sigma=-\frac{2}{3}\frac{e^2}{(2\pi)^3}\int dE\frac{\partial f_0}{\partial E}\int_E dS\frac{\tau v^2}{|\nabla_k E|}, \tag{8}$$

where E is the electron energy and the integration dS is over a constant energy surface, may be written

$$\sigma=-\int dE\,\sigma(E)(\partial f_0/\partial E) \tag{9}$$

defining the function $\sigma(E)$. One then attempts to specify only the behavior of $\sigma(E)$ and does not deal separately with the density of states and the relaxation time. The function $\sigma(E)$ is transformed into another function $\sigma(\epsilon)$ by the substitution $E=kT\epsilon+\zeta$. Klemens[30] has shown that if the transport properties in the presence of a temperature gradient are describable in terms of the same function $\sigma(\epsilon)$ (equivalent to the assumption of the existence of a unique relaxation time) then the Seebeck coefficient S and the Lorenz number L are given by

$$S=(k/e)(K_1/K_0) \tag{10}$$

$$L=\frac{\kappa_e}{\sigma T}=\frac{k^2}{e^2}\left\{\frac{K_2}{K_0}-\left(\frac{K_1}{K_0}\right)^2\right\}, \tag{11}$$

where

$$\sigma=K_0=-\int_{-\infty}^{\infty}\sigma(\epsilon)\frac{\partial f_0}{\partial\epsilon}d\epsilon,$$

$$K_1=-\int_{-\infty}^{\infty}\sigma(\epsilon)\epsilon\frac{\partial f_0}{\partial\epsilon}d\epsilon,$$

$$K_2=-\int_{-\infty}^{\infty}\sigma(\epsilon)\epsilon^2\frac{\partial f_0}{\partial\epsilon}d\epsilon.$$

Therefore, if $-\sigma(\epsilon)(\partial f_0/\partial\epsilon)$ is considered to be a distribution function, then the Seebeck coefficient is proportional to the first moment of this distribution function and the Lorenz number is proportional to the second moment about the mean. This formalism is, of course, simply another way of writing the familiar expression for σ, S, and L. It emphasizes the necessary correlation between these quantities. In dealing with materials for which one has little or no information about the effective masses and/or the scattering processes it permits the extraction of some information from experimental results without making specific assumptions about the effective masses and relaxation times.

The $\sigma(E)$ curve for a p-type semiconductor with a single parabolic valence band and $\tau\propto(E_0-E)^{-\frac{1}{2}}$, where E_0 is the energy of the band edge, is

$$\sigma(E)=0 \qquad E>E_0$$

$$\sigma(E)=a(E_0-E) \qquad E<E_0,$$

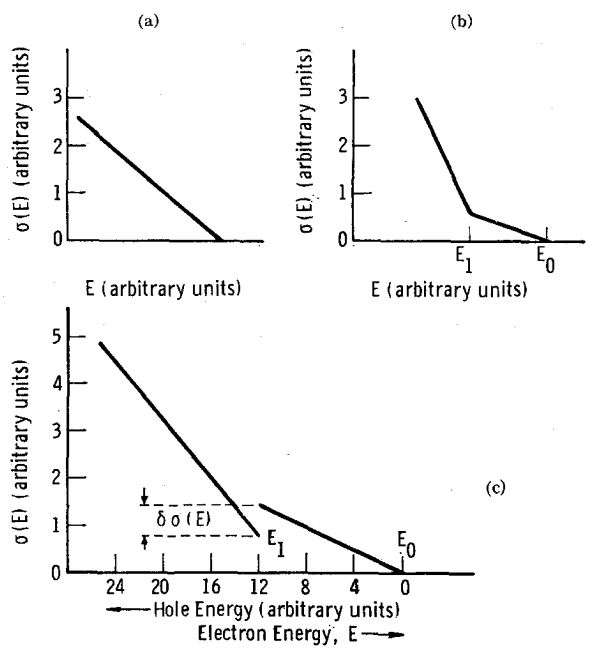

FIG. 6. $\sigma(E)$ function as defined by Eqs. (8) and (9). (a) A standard valence band with $\tau=\tau_0E^{-\frac{1}{2}}$; (b) two overlapping valence bands whose edges are separated by an energy E_1-E_0, $\tau\propto E^{-\frac{1}{2}}$ for both bands; (c) the $\sigma(E)$ function used in this discussion of the transport properties of SnTe.

[28] Ref. 4; see also Ref. 6.

[29] A. H. Wilson, *Theory of Metals* (Cambridge University Press, London, 1953), 2nd ed., p. 197.

[30] P. G. Klemens, *Proceedings of the 4th Conference on Thermal Conductivtiy, San Francisco, 1964* (U. S. Naval Radiological Defense Lab., San Francisco, 1964), Paper 1A. Equation (10) does not include a phonon-drag contribution. It does not seem likely that this is important for SnTe for $T>100$°K because: (1) $\theta\approx130$ °K, and (2) the carrier concentrations are large.

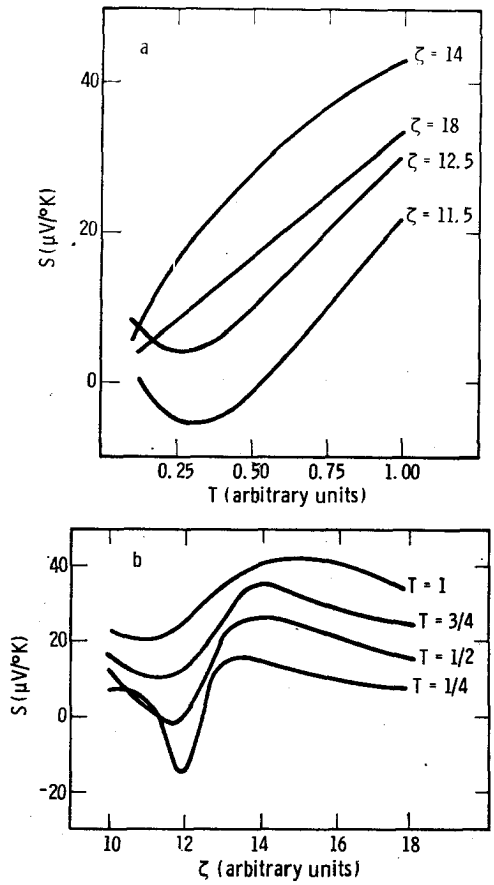

FIG. 7. Calculated values of the Seebeck coefficient, S, using Eq. (10) and the $\sigma(E)$ function shown in Fig. 6(c) plotted against (a) temperature T, (b) Fermi energy ζ, both T and ζ in the arbitrary units of energy shown in Fig. 6(c).

where a may be temperature dependent. As usual in dealing with an extrinsic semiconductor one assumes that $\partial f_0/\partial E$ is such that no other bands need be considered. This $\sigma(E)$ curve is shown in Fig. 6(a). Figure 6(b) shows the $\sigma(E)$ curve for a p-type semiconductor with two overlapping parabolic valence bands, the band edges being separated by an energy E_0-E_1. This is the model treated by Brebrick and Strauss.[15] As previously mentioned, it does not give a good quantitative account of the dependence of the Seebeck coefficient on hole concentration. Therefore, some of the available experimental information is used to modify this model.

There are two experimental results that seem most important: (1) the minimum value of S as a function of hole concentration is almost zero ($S_{\min}\sim 0.5\ \mu$V/°K at 200°K), and (2) the electrical conductivity at 77°K as a function of hole concentration has a local minimum value[12] at very nearly the same hole concentration for which S has its minimum value. Both results can be explained if the $\sigma(E)$ function has a local minimum value for some value of E below E_0. This local minimum must be fairly sharp so that there will be no minimum in a plot of σ vs p at high temperatures where $\partial f_0/\partial E$ must be wide enough to smear out the minimum in $\sigma(E)$. Therefore, although $d\sigma(E)/dE$ should be negative for a valence band [Fig. 6(a)], one must expect $d\sigma(E)/dE$ to be positive over a small range of values of E. Since $\partial f_0/d\epsilon$ is an even function of ϵ only the odd part of $\sigma(\epsilon)$ will enter into K_1, and to first order, K_1 and thus S, will be proportional to some average value of $d\sigma(E)/dE$ (for a highly degenerate metal the relation $S\propto[(d/dE)\ln\sigma(E)]_{E=\zeta}$ is well known). When the Fermi level falls near the minimum in the $\sigma(E)$ curve, the positive and negative values of $d\sigma(E)/dE$ will tend to cancel and the Seebeck coefficient will be small. The simplest function having these properties is shown in Fig. 6(c). If the two-valence-band model is correct, then the abrupt change in $\sigma(E)$ at $E=E_1$ must be ascribed to the effect of a scattering mechanism.

This function is, of course, overly simplified. However, it is very convenient since all the integrals entering into Eqs. (10) and (11) are of the form

$$\int_{\epsilon_a}^{\epsilon_b} \epsilon^n \frac{\partial f_0}{\partial \epsilon} d\epsilon,$$

which is easily evaluated numerically. As we shall see, it is quite adequate for a semiquantitative discussion of the Seebeck coefficient and Lorenz number. This $\sigma(E)$ function is specified by the following parameters: $d\sigma/dE=a$ for $E>E_1$, $d\sigma/dE=b$ for $E<E_1$, $\Delta=E_0-E_1$, and $\delta\sigma(E)$, which for convenience is also written as $(1-c)a\Delta$, where c is a parameter [see Fig. 6(c)]. The values of S and L depend on b/a, c, and Δ. Henceforth, all energies are measured in °K.

Values of b/a, c, Δ, and the energy-scale factor which will convert the arbitrary energy unit used in Fig. 6 into °K can be determined by fitting the experimental values of S to those calculated from Eq. (10) as a function of ζ and T under the following assumptions:

(1) As in the two-valence-band model, p is a monotonically increasing function of ζ.

(2) Not only is the function form of $\sigma(E)$ independent of T and [V_{Sn}] but b/a, c, and Δ are constant.

(3) The temperature dependence of ζ may be ignored.

Thus we attempt to ascribe the major features of the temperature and hole concentration dependence of S to the shape of the $\sigma(E)$ curve and the variation of $\partial f_0/\partial E$ with temperature. Figures 7(a) and 7(b) show the calculated values of S plotted against ζ and T (both ζ and T in arbitrary units) for $b/a=3$ and $c=0.4$. Apart from the negative values of S which are not observed experimentally, comparison of Fig. 7(a) with Fig. 2 shows that the calculation yields values of S in excellent qualitative agreement and rough quantitative agreement with the experimental results if the energy-scale factor is chosen to be about 400, i.e., $T=1$ corresponds to 400°K and $\Delta=4800$°K. Figure 7(b) should be compared to Fig. 1 of Ref. 13 and Fig. 4 of Ref. 12.

This value of Δ is almost exactly equal to the separation between the two valence-band edges suggested by Brebrick and Strauss. Figure 8 shows the quantity σ/akT plotted against ζ. As anticipated, this calculation leads to a minimum in the electrical conductivity as a function of p. However, it suggests that this minimum should become more pronounced at lower temperature, whereas the experimental results show no minimum in the electrical conductivity at 4.2°K as a function of hole concentration. The simplest way to correct this deficiency is to allow c to increase towards 1 as the temperature decreases, i.e., $\delta\sigma(E)$ vanishes. This not only eliminates the minimum in σ but helps eliminate the negative values of S at low temperatures when $\zeta \approx E_1$.

Figure 9 shows values of L calculated from Eq. (11) again using $b/a=3$ and $c=0.4$. Two qualitative features of these curves should be noted: (1) L is an increasing function of temperature, and (2) L has a well-defined maximum value for some value of ζ just smaller than E_1. It is now possible to give a good qualitative account of the measured values of κ shown in Fig. 3. For all samples, κ is rather insensitive to temperature. This is a result of two factors. First, due to the strong point-defect scattering, κ_L varies as approximately $T^{-\frac{1}{2}}$ rather than T^{-1}. Second, the Lorenz number is an increasing function of T so that κ_e increases with temperature. At high temperatures the thermal conductivity of samples b and c is appreciably larger than that of sample a even though all three samples have nearly the same electrical conductivity and the concentration of point defects is larger in samples b and c. This is a result of unusually large values of L, especially for sample b. In Fig. 9, $(\kappa-\kappa_L)/\sigma T$ is plotted against T, where κ and σ are the measured thermal and electrical conductivities and κ_L is computed from Eq. (3). It is seen that this $\sigma(E)$ curve even yields a rough quantitative agreement with the experimental results.

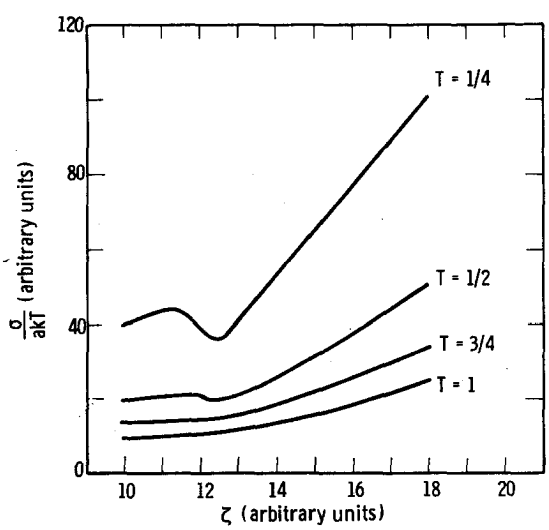

FIG. 8. Calculated values of σ/akT using the $\sigma(E)$ function shown in Fig. 6(c) plotted against ζ. Both σ and ζ are in the arbitrary units shown in Fig. 6(c).

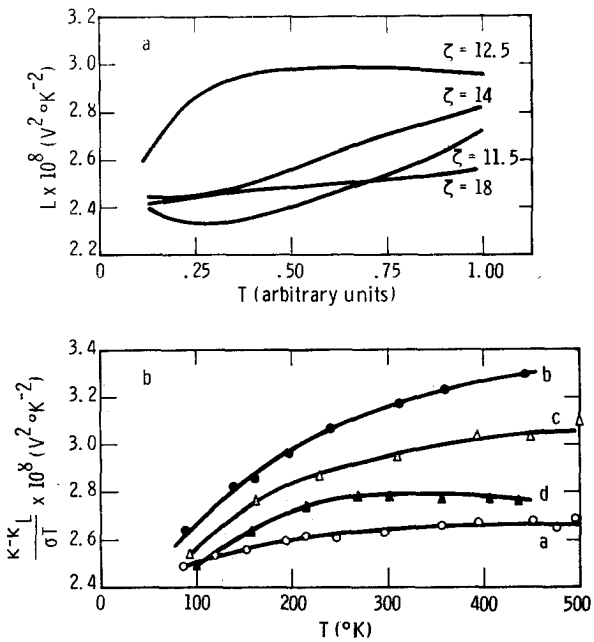

FIG. 9. (a) Calculated values of $L=\kappa_e/\sigma T$ using Eq. (11) and the $\sigma(E)$ function shown in Fig. 6(c) plotted against T in the arbitrary units shown in Fig. 6(c). (b) Values of $(\kappa-\kappa_L)/\sigma T$ plotted against T. κ is the measured thermal conductivity, σ is the measured electrical conductivity, and κ_L is the lattice thermal conductivity calculated from Eq. (3).

Ideally one should like to use the measured values of κ_e to deduce some information about the second moment of $-\sigma(\epsilon)(\partial f_0/\partial\epsilon)$. However, this depends upon making an accurate separation of κ into κ_e and κ_L. While it has been shown that Klemens' theory probably gives reasonably good values for κ_L, one certainly cannot trust the theory to yield accurate values. No pretense is made that the $\sigma(E)$ curve used in these calculations is realistic; in particular, the discontinuity and assumptions 2 and 3 are unrealistic. Nevertheless, we have been able to calculate values of S that are in fair agreement with measured values. Moreover, considering σ, S, and L as functions of p or ζ at fixed T, this model predicts that $P_{\alpha\text{-min}}<P_{\sigma\text{-min}}<P_{L\text{-max}}<P_{\alpha\text{-max}}$, where $P_{\alpha\text{-min}}$ is the value of p for which α has its minimum value, etc. This prediction is in good agreement with the experimental results. We claim that no matter what model of the band structure and the scattering mechanisms may be devised to explain the electrical conductivity and Seebeck coefficient, this model will *necessarily* yield values of L which will vary with T and ζ in a similar fashion to those shown in Fig. 9.

The $\sigma(E)$ curve can easily be made more realistic, the discontinuity may be smoothed out, and by considering specific models of the band structure and scattering mechanisms, the values of a and b may be made to vary with T and $[V_{Sn}]$. There would seem to be little value

in doing this until the discontinuity in the $\sigma(E)$ curve can be explained. Using the two-valence-band model of Brebrick and Strauss in which the effective mass of the holes in the band with the higher *hole* energies was about ten times greater than the effective mass of the holes in the first valence band, one could suppose that interband scattering would be the necessary additional scattering mechanism as suggested by Houston and Allgaier.[11] It is easily seen that the discontinuity in the $\sigma(E)$ curve may describe the effect of interband scattering in a crude way, i.e., the mobility of the light-mass holes is substantially reduced when the light-mass holes can be scattered into heavy mass states. Moreover, recognizing the effectiveness of heavy-mass carriers in screening charge centers as pointed out by Robinson and Rodriguez,[31] one could argue that the effect of the interband scattering should become of less importance at low temperatures where impurity scattering would dominate. The Shubnikov–De Haas oscillations in SnTe observed by Burke *et al.*[14] show that there is indeed a second valence band; however, the effective mass of the carriers in this band is very small. If this should be the only other valence band, then interband scattering[32] cannot be used to explain the experimental results.

SUMMARY AND CONCLUSIONS

The measured thermal conductivity of SnTe has been separated into a lattice and an electronic thermal conductivity. The lattice thermal conductivity can be described by a theory due to Klemens which treats the phonons as being scattered both by umklapp processes and point-defect scattering with the following conclusions:

(1) The lattice thermal conductivity of pure stoichiometric SnTe for $T>100°K$ should be about $13T^{-1}$ $W\cdot cm^{-1}\ °K^{-1}$.

(2) Phonon scattering by the Sn vacancies is strong. Most of this scattering is due to the strain field surrounding the vacancy.

The electronic thermal conductivity has been discussed in terms of a formalism that emphasizes the necessary correlations between the electrical conductivity, Seebeck coefficient and the electronic thermal conductivity. Assuming that the two-valence-band model provides a correct description of the basic features of the band structure and using the function $\sigma(E)$ defined by Eqs. (8) and (9) we conclude that:

(1) The existence of a minimum in σ as a function of p at 77°K implies that $\sigma(E)$ must also have a local minimum value below the edge of the first valence band.

(2) The existence of both a minimum and a maximum in S as a function of p is a consequence of the necessity of having both positive and negative values of $d\sigma(E)/dE$.

(3) The Lorenz number for a material characterized by such a function $\sigma(E)$ must have a maximum value as a function of p. Qualitatively the measured values of the thermal conductivity show that this is the case for SnTe.

Quantitatively fair agreement with the measured values of S can be obtained using an overly simplified function $\sigma(E)$. This function also yields values of L that appear to be in reasonable agreement with the experimental results. The mechanism responsible for this function remains unexplained. If the two-valence-band model is correct, then one must assume that some scattering mechanism reduces the mobility of the holes whose energies lie above an energy that is very close to the edge of the second valence band. The data also suggest that this scattering mechanism is more effective at 300°K than at 100°K.

ACKNOWLEDGMENTS

The author is indebted to Dr. P. G. Klemens, Dr. A. Sagar, and Dr. R. C. Miller for helpful discussions, to Miss B. Kagle for computer programming, and to P. Piotrowski for assistance with the measurements.

[31] J. E. Robinson and S. Rodriguez, Phys. Rev. **135**, A779 (1964).

[32] Recent measurements show that the Nernst–Ettingshausen coefficients for SnTe samples with p near 2×10^{20} cm^{-3} are unusually large, thus indicating the presence of a scattering mechanism which has a strong dependence on the energy of the carriers: B. A. Efimova, V. I. Kaidanov, B. Ya. Moizhes, and I. A. Chernik, Soviet Phys.—Solid State **7**, 2032 (1966).